THE JOURNAL OF BIOLOGICAL CHEMISTRY VOL. 288, NO. 20, pp. 13988–13999, May 17, 2013

Molecular Mediators for Raft-dependent Endocytosis of Syndecan-1, a Highly Conserved, Multifunctional Receptor*[S]

Received for publication, December 12, 2012, and in revised form, March 8, 2013 Published, JBC Papers in Press, March 22, 2013, DOI 10.1074/jbc.M112.444737

Keyang Chen and Kevin Jon Williams[1]

From the Division of Endocrinology, Department of Medicine, Temple University School of Medicine, Philadelphia, Pennsylvania 19140

Background: Endocytosis via rafts remains incompletely characterized.
Results: Raft-dependent endocytosis of syndecan-1 occurs in two phases, each requiring a kinase and a corresponding cytoskeletal partner. Each phase depends on MKKK, a novel, conserved motif within syndecan-1.
Conclusion: These findings demonstrate the molecular choreography behind endocytosis of a raft-dependent receptor.
Significance: Syndecans mediate uptake of biologically and medically important ligands.

Endocytosis via rafts has attracted considerable recent interest, but the molecular mediators remain incompletely characterized. Here, we focused on the syndecan-1 heparan sulfate proteoglycan, a highly conserved, multifunctional receptor that we previously showed to undergo raft-dependent endocytosis upon clustering. Alanine scanning mutagenesis of three to five consecutive cytoplasmic residues at a time revealed that a conserved juxtamembrane motif, MKKK, was the only region required for efficient endocytosis after clustering. Endocytosis of clustered syndecan-1 occurs in two phases, each requiring a kinase and a corresponding cytoskeletal partner. In the initial phase, ligands trigger rapid MKKK-dependent activation of ERK and the localization of syndecan-1 into rafts. Activation of ERK drives the dissociation of syndecan-1 from α-tubulin, a molecule that may act as an anchor for syndecan-1 at the plasma membrane in the basal state. In the second phase, Src family kinases phosphorylate tyrosyl residues within the transmembrane and cytoplasmic regions of syndecan-1, a process that also requires MKKK. Tyrosine phosphorylation of syndecan-1 triggers the robust recruitment of cortactin, which we found to be an essential mediator of efficient actin-dependent endocytosis. These findings represent the first detailed characterization of the molecular events that drive endocytosis of a raft-dependent receptor and identify a novel endocytic motif, MKKK. Moreover, the results provide new tools to study syndecan function and regulation during uptake of its biologically and medically important ligands, such as HIV-1, atherogenic postprandial remnant lipoproteins, and molecules implicated in Alzheimer disease.

There has been considerable recent interest in the molecular participants in raft-mediated endocytosis to compare and contrast with uptake via coated pits (1–4). A broad search identified a set of kinases and structural proteins involved in the endocytosis of simian virus 40 (SV40)[2] (5), a ligand that enters via caveolar and noncaveolar rafts for delivery to the endoplasmic reticulum, bypassing canonical endosomes and lysosomes (6, 7). Nevertheless, although the features of numerous coated pit receptors that allow recruitment of endocytic machinery have been identified (8–10), the characteristics of specific raft receptors that trigger endocytosis have not been defined, not even for SV40 receptors (7).

For several reasons, we focused on the syndecan-1 heparan sulfate proteoglycan (HSPG) as an attractive system to investigate molecular determinants of raft-mediated endocytosis. First, we previously reported that the syndecan-1 HSPG directly mediates the internalization and lysosomal delivery of ligands through a novel endocytic pathway via rafts, independent from coated pits (11, 12). By several criteria, endocytosis via syndecan was identical with endocytosis via a chimeric receptor, FcR-Synd1, that consists of the ectodomain of the IgG Fc receptor Ia linked to the transmembrane and cytoplasmic domains of human syndecan-1, thereby indicating a dependence on these domains. Efficient endocytosis by this pathway is triggered by clustering of syndecan-1 or the chimera. Syndecan-1 clustering would be expected upon binding a multivalent ligand, such as a virus or a lipoprotein. Clustering of the syndecan transmembrane and cytoplasmic domains causes energy-independent movement into cholesterol-rich and detergent-insoluble membrane rafts within 10 min, a necessary step before endocytosis. Uptake into the cell proceeds with a $t_{1/2}$ of 1 h and requires an unspecified tyrosine kinase activity and intact actin microfilaments (11, 12).

The second reason to focus on syndecan-1-mediated endocytosis is that cell-surface HSPGs, including syndecan-1, participate in the catabolism of a number of important ligands, including infectious agents, harmful atherogenic lipoproteins,

* This work was supported, in whole or in part, by National Institutes of Health Grants HL73898 and HL94277. This work was also supported by generous recruitment funds from the Temple University School of Medicine and the Ruth and Yonatan Ben-Avraham Fund.
[S] This article contains supplemental Figs. I–III and Tables I and II.
[1] To whom correspondence should be addressed: Section of Endocrinology, Diabetes, and Metabolism, Temple University School of Medicine, 3322 North Broad St., Medical Office Bldg., Rm. 205, Philadelphia, PA 19140. Tel.: 215-707-4746; Fax: 215-707-5599; E-mail: kjwilliams@temple.edu.

[2] The abbreviations used are: SV40, simian virus 40; FcR-Synd1, chimera of the ectodomain of IgG Fc receptor Ia linked to the transmembrane and cytoplasmic domains of human syndecan-1; HSPG, heparan sulfate proteoglycan; IB, immunoblot; IP, immunoprecipitation; LpL, lipoprotein lipase; mLDL, methylated low density lipoprotein; SCD1, syndecan-1; ANOVA, analysis of variance; UM, unmutated.

enzymes, growth factors, platelet secretory products, and proteins implicated in Alzheimer disease (11, 13–17). Exploring the molecular mechanisms for syndecan-1-mediated endocytosis will substantially advance our understanding of how cells handle these biologically and medically significant ligands.

Third, the transmembrane and cytoplasmic domains of human syndecan-1 are highly conserved, indicating key essential functions. These domains show over 50% aminoacyl identity with the sole *Drosophila* syndecan, indicating a remarkable degree of preservation during half a billion years of evolution (18). Thus, the endocytic determinants and intracellular partners of syndecan-1 are likely to have broad significance.

Based on sequence alignments, the syndecan-1 cytoplasmic tail has been divided into the first conserved region (C1), the variable domain (V), and the second conserved region (C2) (Fig. 1*A*) (14, 19, 20). Each of these cytoplasmic portions has been shown to interact with specific intracellular binding partners and to mediate several cellular functions, although none are directly related to the process of endocytosis. Previous studies indicate that three regions interact with the cytoskeleton, namely the second half of C1 (21), the V-domain (22), and the terminal C2 domain (14, 23, 24). Moreover, C2 controls syndecan recycling after endocytosis (25).

In this study, we sought to identify determinants within the syndecan-1 cytoplasmic tail, as well as their intracellular partners, that mediate efficient endocytosis upon clustering. Surprisingly, this work implicates none of the known cytoskeleton-interacting domains of syndecan-1 in the endocytosis of multivalent ligands. Instead, we identified a single, conserved juxtamembrane motif, MKKK, in the syndecan-1 cytoplasmic tail that mediates the sequential activation of two kinases, ERK and then Src. Upon activation, the two kinases each control the interaction of syndecan-1 with two key cytoskeletal molecules to mediate efficient endocytosis. Portions of this work were presented at the 2008 and 2011 American Heart Association Scientific Sessions (26, 27).

EXPERIMENTAL PROCEDURES

Molecular Methods—Our FcR-Synd1 chimera was previously described (11, 12); now it is expressed in the pcDNA3.1 plasmid (Invitrogen). Alanine scanning mutagenesis of the syndecan-1 cytoplasmic tail within FcR-Synd1 was performed with the QuikChange kit (catalog no. 200518, Stratagene-Agilent Technology, Santa Clara, CA), using our unmutated FcR-Synd1 expression plasmid as template and the mutagenesis primers listed in supplemental Table I. All mutants were sequenced to verify the introduction of DNA changes. McArdle 7777 rat hepatoma cells were obtained from the American Type Culture Collection (Manassas, VA; catalog no. CRL-1601) and cultured as described previously (16, 28). The unmutated FcR-Synd1 plasmid, all mutant plasmids, and the empty pcDNA3 vector were transfected one at a time into McArdle cells, using the FuGENE 6 reagent (Roche Applied Science). Stably expressing clones were selected with G418, followed by verification of expression by immunoblots of whole-cell homogenates using anti-FcR antibodies. To assess cell-surface display of the chimera and its mutants, we measured cell-surface binding of ligand, *i.e.* ^{125}I-labeled nonimmune human IgG (unlabeled IgG purchased from Rockland Immunochemicals, Gilbertsville, PA, catalog no. 009-0102, and then radioiodinated). To avoid receptor internalization or recycling, this particular assay was performed entirely at 4 °C.

Cell Culture, Ligand Catabolism, and Protein Analyses—Raft localization and internalization of ^{125}I-labeled IgG by cells expressing the unmutated parental FcR-Synd1 chimera and the alanine scanning mutants were performed following our published protocols (11, 12). In brief, the ligand for FcR-Synd1, ^{125}I-labeled nonimmune human IgG, was bound at 4 °C to the surface of these McArdle cell lines. Unbound material was washed away, and then the cells were incubated for 5–60 min at 37 °C, in the absence or presence of our clustering agent (goat $F(ab')_2$ against human IgG Fab; Rockland Immunochemicals, catalog no. 709-1118). Raft localization was assessed by cold Triton insolubility and internalization by resistance to an acid wash that releases surface-bound IgG. To assess the syndecan-1 HSPG itself, we used untransfected McArdle cells, which express this molecule endogenously (16). We used model remnant lipoproteins as ligands for syndecan-1, as described (11, 16, 29). Model remnant lipoproteins were prepared by adding lipoprotein lipase (LpL), a key protein on remnants recognized by HSPGs, to unlabeled or ^{125}I-labeled human LDL that we had methylated to an extent that blocks its binding to LDL receptors (mLDL), thereby mimicking $apoB_{48}$ (11, 29).

Cellular extractions, immunoprecipitations, co-immunoprecipitations, immunoblots, and siRNA knockdowns were performed following our published protocols (16, 28). Antibodies against target molecules (total target as well as forms with site-specific phosphorylations) are listed in supplemental Table II. The nontarget siRNA pool, designed and microarray tested by the manufacturer for minimal targeting of rat genes, and the siRNA pool against rat cortactin were from Dharmacon (Lafayette, CO; catalog nos. D-001910-10-20 and L-080141-01-0010, respectively).

Statistical Analyses—Quantitative data from our experiments were analyzed using SigmaStat version 3 (SPSS Inc., Chicago). Normally distributed data are reported as the mean ± S.E., $n = 3$ per group per experiment. For comparisons between a single experimental group and a control, Student's unpaired two-tailed t test was used. For comparisons involving several groups simultaneously, analysis of variance (ANOVA) was initially used, followed by pairwise comparisons of each experimental group *versus* the control group by the Dunnett q' statistic.

RESULTS

Alanine Scanning Mutagenesis Identifies a Single Highly Conserved Juxtamembrane Motif, MKKK, in the Syndecan-1 Cytoplasmic Tail as Essential for Efficient Endocytosis after Clustering—We embarked on a comprehensive survey of the syndecan-1 cytoplasmic tail using alanine scanning mutagenesis. Our mutations, displayed in Fig. 1*A*, tampered with only 3–5 consecutive aminoacyl residues at a time. To avoid interference from the native unmutated syndecan-1 HSPG, particularly during clustering, the mutations were introduced into the FcR-Synd1 chimera, and hence we used nonimmune human IgG as the ligand. We covered the entire

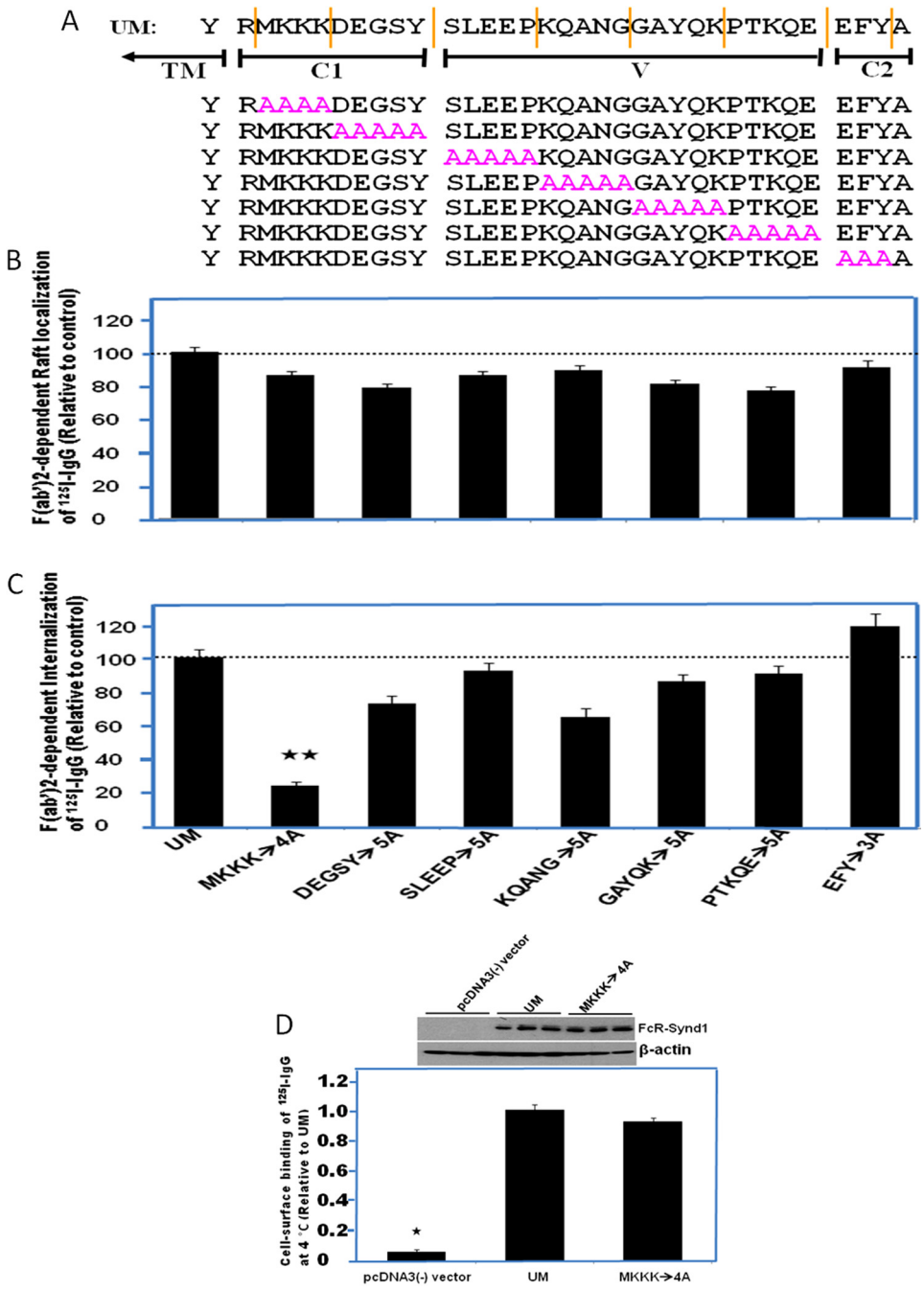

FIGURE 1. **Alanine scanning mutagenesis identifies a single highly conserved juxtamembrane motif, MKKK, in the syndecan-1 cytoplasmic tail as essential for efficient endocytosis after clustering.** *A,* native unmutated (*UM*) and mutated syndecan-1 sequences. *Top sequence* shows the final transmembrane (*TM*) aminoacyl residue and the entire cytoplasmic tail of syndecan-1. These regions form the C terminus of the UM FcR-Synd1 chimera. The first conserved (*C1*), variable (*V*), and second conserved (*C2*) domains of the syndecan-1 cytoplasmic tail are indicated. *Lower sequences* show the C-terminal aminoacyl residues of each of our alanine scanning mutants of the FcR-Synd1 chimera. Mutated residues are indicated in *purple*. We designated each mutant construct by the short sequence that was replaced by an equal number of alanines (*e.g.* MKKK→4A and DEGSY→5A). The UM and mutant constructs were expressed, one at a time, in McArdle 7777 hepatoma cells, followed by analysis of ligand catabolism. *B* and *C,* raft localization and internalization triggered by clustering. The ligand for FcR-Synd1, ^{125}I-labeled nonimmune human IgG, was bound at 4 °C to the surface of the McArdle cell lines described in *A*. Unbound material was washed away, and then the cells were incubated for 1 h at 37 °C in the absence or presence of our clustering agent (goat F(ab′)$_2$ against human IgG Fab). Raft localization was assessed by cold Triton insolubility and internalization by resistance to an acid wash that releases surface-bound IgG. Displayed are clustering-dependent raft localization (*B*) and internalization of ligand (*C*), normalized to control values from cells expressing the unmutated chimera (mean ± S.E., $n = 3$). Non-normalized control values were 433.91 ± 26.24 ng/mg that moved into rafts and 416.38 ± 14.15 ng/mg that became internalized (total cell-associated ligand was 850.29 ± 18.2 ng/mg). The *horizontal dotted lines* represent the mean values from UM FcR-Synd1-expressing cells. *B*, $p > 0.5$ by ANOVA. *C*, *, $p < 0.01$ by ANOVA; **, $p < 0.01$ compared with the UM value by the Dunnett test. The data are representative of a total of three independent catabolism experiments. Because of the importance of the MKKK→4A mutant, the upper image in *D* shows, side-by-side, an anti-FcR immunoblot in triplicate of McArdle 7777 hepatoma cells transfected with an empty vector (*pcDNA3*(−)) or expressing the unmutated FcR-Synd1 chimera or the MKKK→4A mutant. The *column graph* in the lower part of *D* shows cell-surface binding of ^{125}I-labeled IgG by the same three types of transfected hepatoma cells. To specifically assess cell-surface display of the unmutated and MKKK→4A constructs, this assay was performed entirely at 4 °C to block internalization or recycling. In the *column graph* of *D*, $p < 0.01$ by ANOVA; *, $p < 0.01$ compared with the UM value by the Dunnett test.

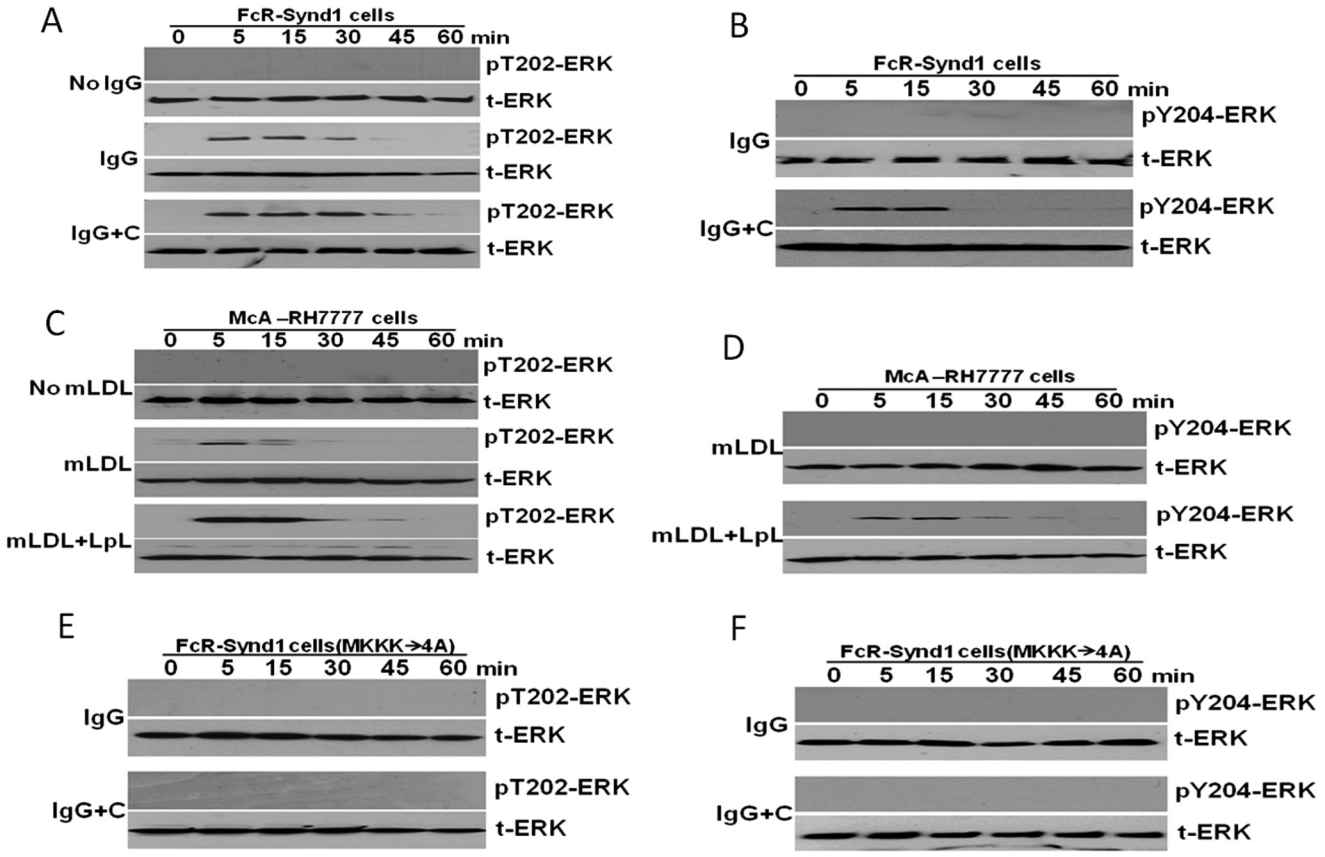

FIGURE 2. **MKKK motif mediates rapid ERK activation upon ligand binding.** *A* and *B,* phosphorylations of ERK stimulated by ligands for the FcR-Synd1 chimera. McArdle hepatocytes expressing the unmutated FcR-Synd1 chimera were preincubated at 4 °C without or with unlabeled IgG as indicated, unbound material was washed away, and then the cells were incubated at 37 °C for the indicated times, in the absence or presence of our clustering agent (+*C*). Displayed are immunoblots of cellular homogenates for phosphorylations of ERK at Thr-202 (*pT202-ERK*, *A*) and Tyr-204 (*pY204-ERK*, *B*). Immunoblots for total ERK (*t-ERK*, meaning phosphorylated plus unphosphorylated forms) are also shown for each sample. *C* and *D,* phosphorylations of ERK stimulated by ligands for syndecan-1. Untransfected McArdle hepatocytes, which express endogenous syndecan-1, were incubated at 37 °C, without or with mLDL, without or with lipoprotein lipase (+*LpL*), for the indicated times. Displayed are immunoblots for phosphorylated ERK (*C, pT202*; *D, pY204*) and for total ERK. *E* and *F,* MKKK motif mediates ERK activation. McArdle hepatocytes expressing the FcR-Synd1 (MKKK→4A) mutant were treated as in *A*. Displayed are immunoblots for phosphorylated (*E, pT202*; *F, pY204*) and total ERK. The data in this figure are representative of a total of three independent immunoblotting experiments.

syndecan cytoplasmic tail within the FcR-Synd1 chimera, except for the first cytoplasmic residue, Arg (R), which we found to be required for export to the cell surface. The unmutated (UM) parent and mutant constructs were each expressed in McArdle 7777 hepatoma cells, followed by analysis of the catabolism of labeled IgG.

All alanine scanning mutants moved into rafts upon ligand clustering (Fig. 1*B*). Replacement of a highly conserved juxtamembrane motif, MKKK, with four alanines was the only mutation that blocked efficient endocytosis after clustering (Fig. 1*C*). As a control, Fig. 1*D* shows that the MKKK→4A mutant is expressed well and traffics to the cell surface, at similar levels to the unmutated construct. Thus, despite prior reports that other syndecan cytoplasmic domains link to the cytoskeleton (14, 21–24), we found the juxtamembrane MKKK motif to be uniquely critical for this raft- and actin-dependent endocytic pathway.

MKKK Motif Mediates Basal Association with α-Tubulin, Rapid ERK Activation upon Ligand Binding, and Then ERK-dependent Dissociation from α-Tubulin, a Required Step for Efficient Endocytosis—To determine how the MKKK motif mediates endocytosis, we examined its role in several previously reported syndecan functions, even though none of those functions had been known to affect ligand internalization. We began with ERK activation, because it can occur after ligand binding (30) and was reported to be an early event during syndecan-1-mediated internalization (<10 min) (31). Previous studies did not indicate which site(s) on ERK became phosphorylated upon syndecan engagement. Here, we used specific antibodies that distinguish between phosphorylations at Thr-202 and Tyr-204 (Thr(P)-202 and Tyr(P)-204, abbreviated in Fig. 2 as pT202 and pY204) (28). Binding of nonimmune, monomeric IgG to FcR-Synd1, without clustering, triggered phosphorylation at Thr-202 (Fig. 2*A*), whereas clustering was required for the formation of dually phosphorylated ERK (Fig. 2, *A* and *B*). Similarly, addition of methylated LDL (mLDL) to untransfected hepatocytes provoked Thr-202 phosphorylation of ERK (Fig. 2*C*), whereas the further addition of lipoprotein lipase, which converts mLDL into a multivalent ligand for syndecan-1, was required for the formation of dually phosphorylated Thr(P)-202/Tyr(P)-204-ERK (Fig. 2, *C* and *D*). In all cases, ERK phosphorylation was evident by 5 min after addition of ligand. Of note, replacement of the MKKK motif in FcR-Synd1 with four consecutive alanines (MKKK→4A) completely abolished any ERK phosphorylation by either monomeric or multivalent ligands (Fig. 2, *E* and *F*).

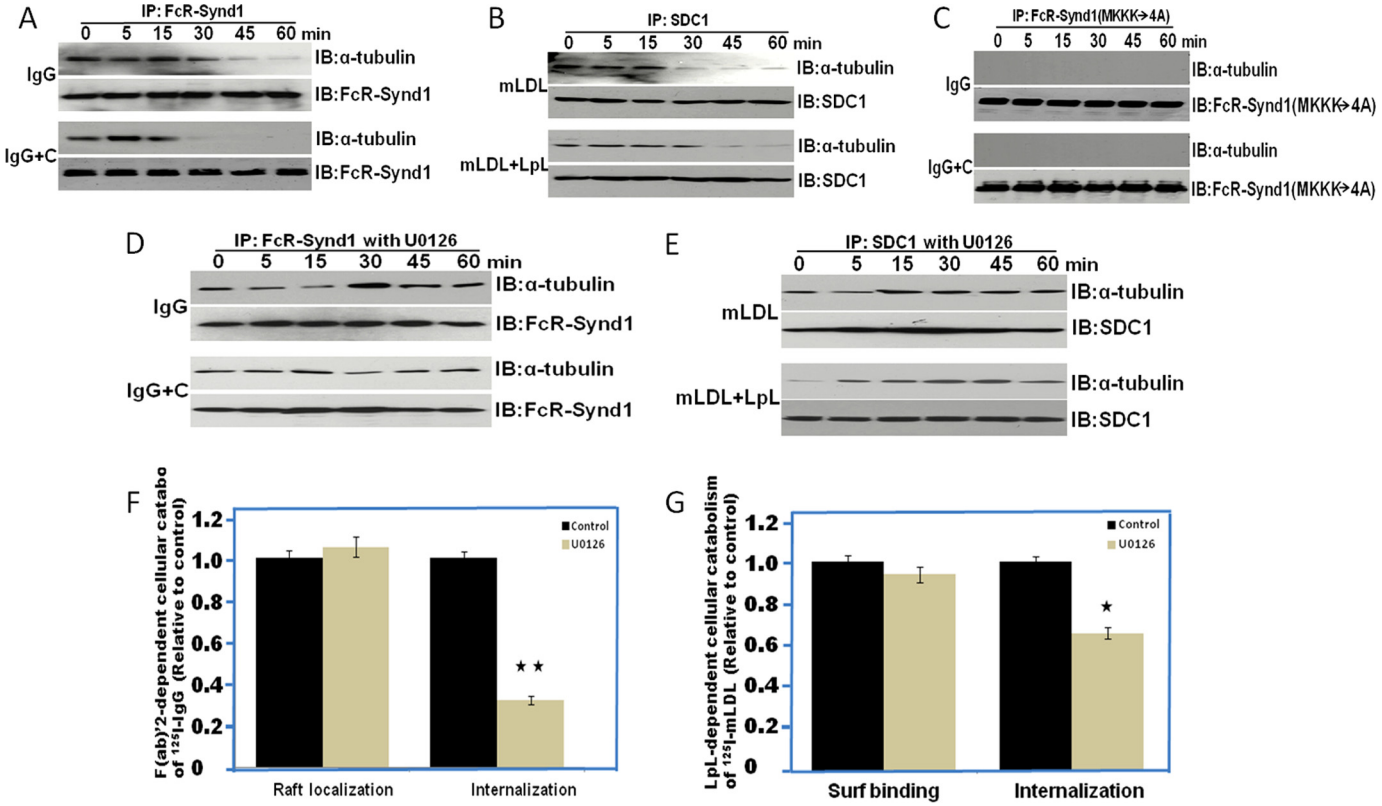

FIGURE 3. **MKKK motif mediates basal association with α-tubulin and then ERK-dependent dissociation from α-tubulin upon ligand binding, a required step for efficient endocytosis.** *A,* basal association of α-tubulin with the FcR-Synd1 chimera, with release after ligand binding. McArdle hepatocytes expressing the unmutated FcR-Synd1 chimera were treated as in Fig. 2, *A* and *B*, followed by extraction into Nonidet P-40, immunoprecipitation with anti-FcR antibodies (*IP: FcR-Synd1*), and then electrophoretic separation. Shown are immunoblots that were performed to detect α-tubulin (*IB: α-tubulin*), and then to verify immunoprecipitation and loading, the same membranes were stripped and reprobed to detect FcR-Synd1 (*IB: FcR-Synd1*). *B,* basal association of α-tubulin with syndecan-1, with release after ligand binding. Untransfected McArdle hepatocytes were treated as in Fig. 2, *C* and *D*, followed by extraction, immunoprecipitation with anti-syndecan-1 antibodies (*IP: SDC1*), and then electrophoretic separation. Shown are immunoblots to detect α-tubulin (*IB: α-tubulin*), and then the same membranes were stripped and reprobed to detect syndecan-1 (*IB: SDC1*). *C,* MKKK motif mediates basal association with α-tubulin. McArdle hepatocytes expressing the FcR-Synd1 (*MKKK→4A*) mutant were treated then analyzed as in *A*. *D,* dissociation of α-tubulin from the FcR-Synd1 chimera requires activation of ERK. McArdle hepatocytes expressing the unmutated FcR-Synd1 chimera were treated and then analyzed as in *A*, except that the incubation at 37 °C included U0126, an inhibitor of ERK. *E,* dissociation of α-tubulin from syndecan-1 requires ERK activation. Untransfected McArdle hepatocytes were treated and then analyzed as in *B*, except that the incubations included U0126, an inhibitor of ERK. *F,* efficient endocytosis of FcR-Synd1 after clustering requires activation of ERK. Raft localization and internalization of ^{125}I-labeled IgG triggered by clustering was assessed after 1 h at 37 °C, as in Fig. 1, using McArdle hepatocytes expressing the unmutated FcR-Synd1 chimera. *Black columns,* without U0126; *tan columns,* with U0126. Displayed are clustering-dependent raft localization and internalization of ligand, normalized to control values from cells without U0126 (mean ± S.E., $n = 3$; non-normalized control values were 496.4 ± 16.23; 570.19 ± 8.06 ng/mg, respectively). **, $p < 0.01$ (two-tailed Student's *t* test). *G,* efficient endocytosis of a multivalent ligand for syndecan-1 requires ERK activation. Untransfected McArdle hepatocytes were incubated for 1 h at 37 °C with ^{125}I-labeled mLDL, without or with LpL, without (*black columns*) or with (*tan columns*) the ERK inhibitor U0126. Displayed are LpL-dependent surface (*Surf*) binding and internalization of ligand, normalized to control values from cells without U0126 (mean ± S.E., $n = 3$; non-normalized control values were 317.63 ± 12.9 and 360.1 ± 9.63 ng/mg, respectively). *, $p < 0.01$ (two-tailed Student's *t* test). The data in this figure are representative of a total of three independent co-immunoprecipitation experiments (*A–E*) and three independent ligand catabolism experiments (*F* and *G*).

A previous report indicated that an affinity column made from a Sepharose-linked peptide corresponding to the cytoplasmic tail of syndecan-3 (neural syndecan) was able to bind α-tubulin, Src family kinases, and cortactin from crude brain homogenates (32). Binding was attributed to the C1 domain of the syndecan-3 peptide (32). Here, to examine a possible association between α-tubulin and the syndecan-1 cytoplasmic tail in our cultured cells, we used co-immunoprecipitations. In the absence of bound ligand, both FcR-Synd1 and native syndecan-1 strongly associated with α-tubulin (Fig. 3, *A* and *B*, *0 min*). Basal association with α-tubulin was entirely dependent on the MKKK motif, thereby pinpointing this function to those four amino acids within the C1 domain (Fig. 3*C*). Surprisingly, addition of ligand provoked the dissociation of FcR-Synd1 and syndecan-1 from α-tubulin within 30–45 min (Fig. 3, *A* and *B*).

These results indicate three new functions for the MKKK motif of the syndecan cytoplasmic tail, namely Thr-202 phosphorylation of ERK (Fig. 2, *A*, *C* and *E*), regulated dissociation from α-tubulin (Fig. 3, *A–C*), and Tyr-204 phosphorylation of ERK (Fig. 2, *B*, *D* and *F*). The first two are triggered by ligand binding and the third by clustering. To determine whether these effects are causally connected, we used the ERK inhibitor U0126. This compound completely blocked the ability of any ligand, either monomeric or multivalent, to provoke the dissociation of FcR-Synd1 or syndecan-1 from α-tubulin (Fig. 3, *D* and *E*). In most of our experiments, ERK inhibition actually enhanced the association between the syndecan cytoplasmic tail and α-tubulin after addition of ligand (Fig. 3, *D* and *E*). To test a role for these processes in syndecan-mediated endocytosis, we found that ERK inhibition significantly interfered with

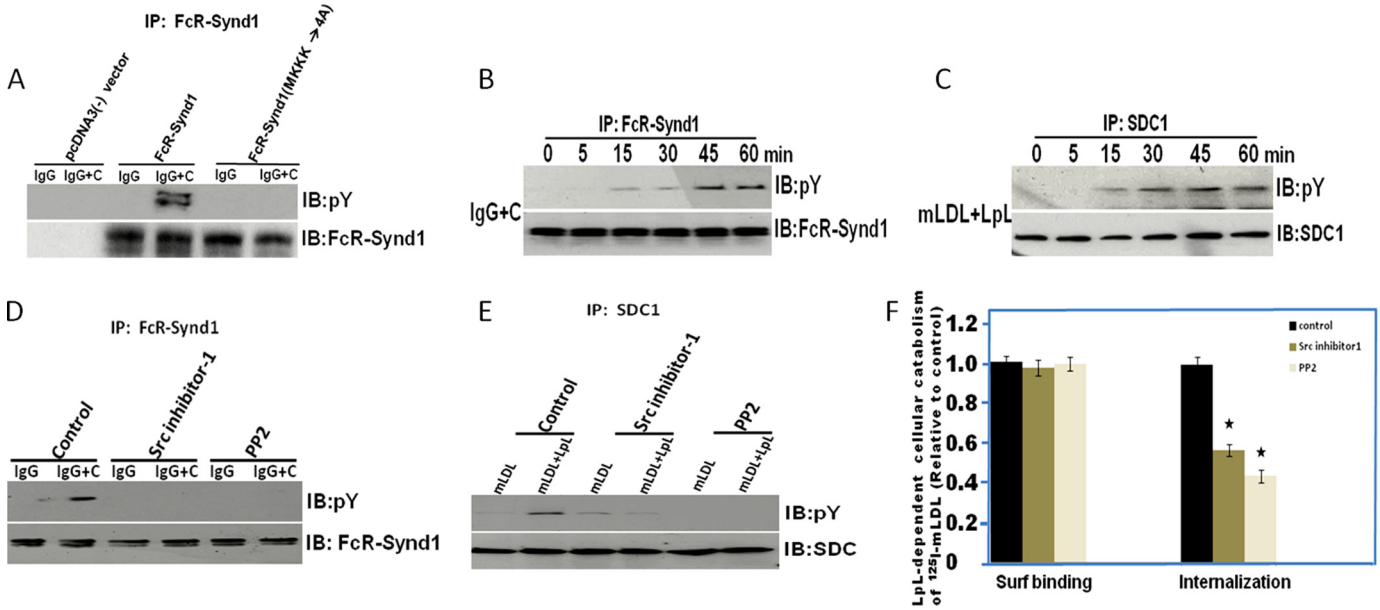

FIGURE 4. **Upon clustering, the MKKK motif gradually triggers Src-dependent tyrosine phosphorylation of the syndecan-1 transmembrane and cytoplasmic domains, which in turn causes efficient endocytosis.** *A,* MKKK-dependent tyrosine phosphorylation of the syndecan-1 cytoplasmic tail after clustering. McArdle hepatocytes transfected with an empty vector (*pcDNA3*(−)) or expressing the unmutated FcR-Synd1 chimera or the MKKK→4A mutant were preincubated at 4 °C without or with unlabeled IgG, as indicated. Unbound material was washed away, and then the cells were incubated at 37 °C for 60 min in the absence or presence of our clustering agent (+*C*). Displayed are immunoprecipitations with anti-FcR antibodies (*IP: FcR-Synd1*), followed by immunoblots with the 4G10 antibody against phosphotyrosine residues (*IB: pY*) or antibodies against the FcR ectodomain, to verify immunoprecipitation (*IB: FcR-Synd1*). *B,* time course of tyrosine phosphorylation of FcR-Synd1 after clustering. McArdle hepatocytes expressing the unmutated FcR-Synd1 chimera were preincubated at 4 °C with unlabeled IgG; unbound material was washed away, and then the cells were incubated in the presence of our clustering agent (+*C*) at 37 °C for the indicated times. Displayed are immunoprecipitations with anti-FcR antibodies (*IP: FcR-Synd1*), followed by immunoblots with antibodies against phosphotyrosine residues (*IB: pY*) or against the FcR ectodomain (*IB: FcR-Synd1*). *C,* time course of tyrosine phosphorylation of syndecan-1 after clustering. Untransfected McArdle hepatocytes, which express endogenous syndecan-1, were incubated with methylated LDL plus lipoprotein lipase (*mLDL+LpL*) at 37 °C for the indicated times. Displayed are immunoprecipitations with anti-syndecan-1 antibodies (*IP: SDC1*), followed by immunoblots with antibodies against phosphotyrosine residues (*IB: pY*) or against syndecan-1 (*IB: SDC1*). *D,* tyrosine phosphorylation of FcR-Synd1 after clustering requires Src family kinases. McArdle hepatocytes expressing the unmutated FcR-Synd1 chimera were treated and then analyzed as in *A*, except that the indicated incubations included Src kinase inhibitors (*Src inhibitor-1* or *PP2*). *E,* tyrosine phosphorylation of syndecan-1 after clustering requires Src family kinases. Untransfected McArdle hepatocytes were incubated for 1 h at 37 °C with mLDL, without or with LpL, without (*Control*) or with Src kinase inhibitors (*Src inhibitor-1* or PP2). Displayed are immunoprecipitations with anti-syndecan-1 antibodies, followed by immunoblots for phosphotyrosines or syndecan-1. *F,* efficient syndecan-1-mediated endocytosis after clustering requires Src family kinases. Untransfected McArdle hepatocytes were incubated for 1 h at 37 °C with ^{125}I-labeled mLDL, without or with LpL, without (*black columns*) or with (*dark* and *light tan columns*) the indicated Src family kinase inhibitors. Displayed are LpL-dependent surface (*Surf*) binding and internalization of ligand, normalized to control values from cells without the inhibitors (mean ± S.E., $n = 3$; non-normalized control values were 404.13 ± 8.6 and 397.1 ± 7.21 ng/mg, respectively). $p < 0.01$ by ANOVA; *, $p < 0.01$ compared with the control value by the Dunnett test. The data are representative of a total of three independent IP/IB experiments (*A–E*) and ligand catabolism experiments (*F*).

internalization of clustered ^{125}I-labeled IgG by FcR-Synd1 and of LpL-enriched ^{125}I-labeled mLDL by syndecan-1 (Fig. 3, *F* and *G*). Thus, activation of ERK is an essential step for efficient syndecan-mediated endocytosis of multivalent ligands, possibly through its role in freeing the MKKK domain from α-tubulin.

Upon Clustering, the MKKK Motif Gradually Triggers Src-dependent Tyrosine Phosphorylation of the Syndecan-1 Transmembrane and Cytoplasmic Domains, Which in Turn Causes the Robust Recruitment of Cortactin and Efficient Endocytosis—We next focused on tyrosine phosphorylations. We previously reported an essential role for an unspecified tyrosine kinase activity in syndecan-mediated endocytosis (11). The syndecan-1 cytoplasmic tail contains four absolutely conserved tyrosyl residues (Fig. 1) (14, 19, 20), and as just noted, the C1 domain of syndecan-3 can bind Src family kinases (32). Here, we found that ligand binding, but only with clustering, provoked tyrosine phosphorylation of the syndecan transmembrane and cytoplasmic domains of the FcR-Synd1 chimera (Fig. 4*A*). Moreover, this effect was entirely abolished by replacement of the MKKK motif with four alanines (Fig. 4*A*). Interestingly, robust tyrosine phosphorylation of FcR-Synd1 and of syndecan-1 after clustering required 45–60 min (Fig. 4, *B* and *C*), *i.e.* it resembles the time course that we had reported for syndecan-1-mediated endocytosis (11, 12). To characterize the enzymes responsible for tyrosine phosphorylation of FcR-Synd1 and syndecan-1 after clustering, we found that the process was blocked by two structurally distinct Src family kinase inhibitors, namely Src inhibitor-1 and PP2 (Fig. 4, *D* and *E*). Moreover, inhibition of Src family kinases impaired syndecan-1-mediated endocytosis (Fig. 4*F*).

We examined potential interactions with cortactin, which is a particularly attractive molecule in this circumstance, because it has been shown to bind filamentous actin and to participate in membrane-cytoskeletal interactions in several circumstances, such as clathrin-dependent and -independent endocytosis (33). Unlike the situation with α-tubulin, however, basal association of FcR-Synd1 and native syndecan-1 with cortactin was low or undetectable by co-immunoprecipitation (Fig. 5, *A* and *B*, *0 min*). Ligand binding, but only with clustering, stimulated the recruitment of cortactin to FcR-Synd1 and syndecan-1 (Fig. 5, *A* and *B*, *lower immunoblots*). Cortactin recruit-

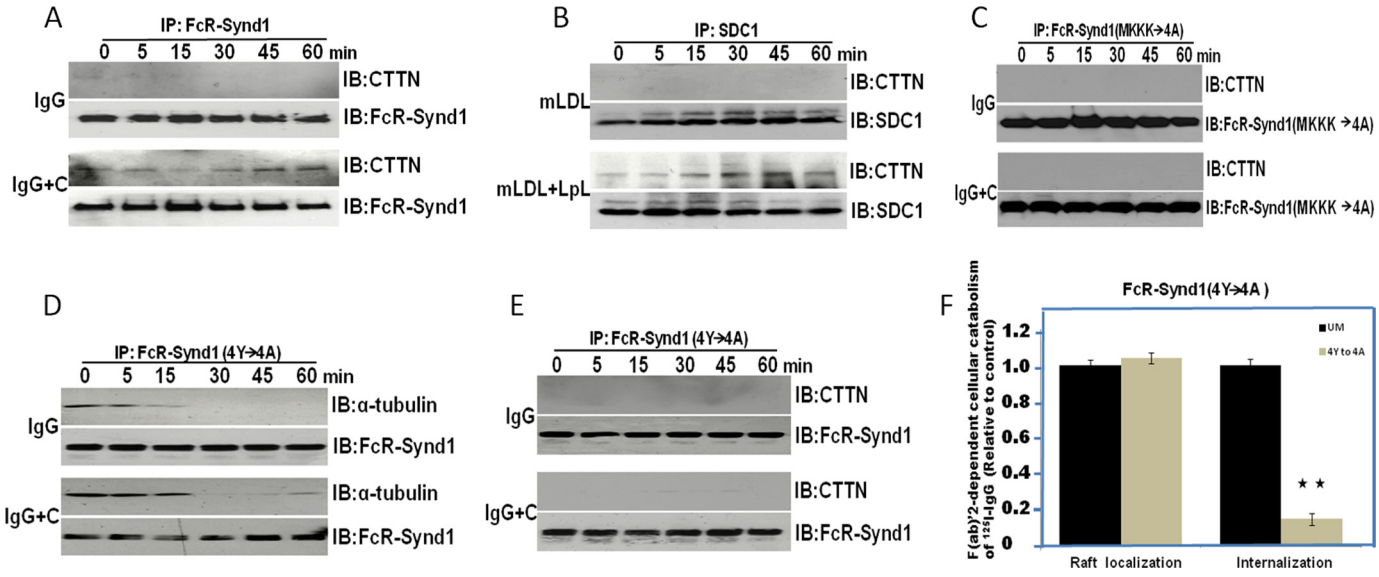

FIGURE 5. **Upon clustering, the MKKK motif gradually recruits cortactin and drives endocytosis, in processes that depend on tyrosines within the syndecan-1 transmembrane and cytoplasmic domains.** *A,* clustering of FcR-Synd1 stimulates the recruitment of cortactin. McArdle hepatocytes expressing the unmutated FcR-Synd1 chimera were treated as in Fig. 2, *A* and *B*. Displayed are immunoprecipitations with anti-FcR antibodies (*IP: FcR-Synd1*), followed by immunoblots for cortactin (*IB: CTTN*) or the FcR ectodomain, to verify immunoprecipitation and loading (*IB: FcR-Synd1*). *B,* clustering of syndecan-1 stimulates the recruitment of cortactin (*CTTN*). Untransfected McArdle hepatocytes were treated as in Fig. 2, *C* and *D*. Displayed are immunoprecipitations with anti-syndecan-1 antibodies, followed by immunoblots for cortactin (*IB: CTTN*) or for syndecan-1 (*IB: SCD1*). *C,* MKKK motif mediates cortactin recruitment after clustering. McArdle hepatocytes expressing the FcR-Synd1 (MKKK→4A) mutant were treated then analyzed as in *A*. *D,* basal association of α-tubulin with the FcR-Synd1 chimera and then release after clustering do not require the four conserved syndecan tyrosyl residues. McArdle hepatocytes expressing the FcR-Synd1 (4Y→4A) mutant were treated as in *A*. Displayed are immunoprecipitations with anti-FcR antibodies (*IP: FcR-Synd1*), followed by immunoblots for α-tubulin (*IB: α-tubulin*) or the FcR ectodomain (*IB: FcR-Synd1*). *E,* recruitment of cortactin after clustering of FcR-Synd1 absolutely depends on the four conserved syndecan tyrosyl residues. McArdle hepatocytes expressing the FcR-Synd1 (*4Y→4A*) mutant were treated then analyzed as in *A*. *F,* efficient endocytosis of FcR-Synd1 after clustering absolutely requires the four conserved syndecan tyrosyl residues. Raft localization and internalization of ^{125}I-labeled IgG triggered by clustering was assessed after 1 h at 37 °C, as in Fig. 1, using McArdle hepatocytes expressing the unmutated FcR-Synd1 chimera (*black columns*) or the 4Y→4A mutant (*tan columns*). Displayed are clustering-dependent raft localization and internalization of ligand, normalized to control values from cells expressing the unmutated chimera (mean ± S.E., $n = 3$; non-normalized control values were 310.51 ± 10.43 and 361.49 ± 9.78 ng/mg, respectively). **, $p <$ 0.001 (two-tailed Student's *t* test). The data are representative of a total of three independent co-immunoprecipitation (*A–E*) and ligand catabolism (*F*) experiments.

ment to FcR-Synd1 and syndecan-1 after clustering also required 45–60 min. Recruitment of cortactin after clustering was entirely dependent on the MKKK motif (Fig. 5*C*).

Thus, tyrosine phosphorylation of syndecan-1, cortactin recruitment, and endocytosis occur with essentially the same time course after clustering. To establish a causal chain, we constructed a new mutant, in which we replaced all four syndecan tyrosines in FcR-Synd1 with alanines. This construct, FcR-Synd1 (4Y→4A), still underwent raft localization upon clustering (data not shown) and loss of tubulin upon ligand binding (Fig. 5*D*), but it failed to undergo tyrosine phosphorylation (supplemental Fig. I), recruitment of cortactin (Fig. 5*E*), or endocytosis after clustering (Fig. 5*F*). Thus, tyrosine phosphorylation, even in the continued presence of the MKKK motif, is required for robust cortactin recruitment and efficient endocytosis. In contrast, inhibition of ERK still allowed cortactin recruitment (supplemental Fig. II, *A* and *B*; compare with Fig. 3, *D–G*).

To independently verify this sequence of events using the unmutated FcR-Synd1 chimera and the syndecan-1 HSPG, we examined each step in the endocytic pathway in the absence *versus* presence of the Src family kinase inhibitor PP2. Inhibition of Src family kinases had no effect on ERK phosphorylation (supplemental Fig. III, *A–D*), raft localization (data not shown), or loss of α-tubulin from FcR-Synd1 or syndecan-1 after addition of multivalent ligands (supplemental Fig. III, *E* and *F*; compare with Fig. 5*D*). Consistent with the ability of PP2 to block tyrosine phosphorylation of FcR-Synd1 and syndecan-1 after clustering (Fig. 4, *D* and *E*), Src family kinase inhibition also stopped the recruitment of cortactin, as assessed by co-immunoprecipitations (supplemental Fig. III, *G* and *H*; compare with Fig. 5*E*). As noted above and in Fig. 4*F*, inhibition of Src family kinases interfered with endocytosis of multivalent ligands, *i.e.* similar to the effect of the 4Y→4A mutation (Fig. 5*F*).

Cortactin Is Required for Rapid Syndecan-mediated Activation of ERK upon Ligand Binding, ERK-dependent Dissociation from α-Tubulin, and Efficient Endocytosis of FcR-Synd1 and Syndecan-1 after Clustering, but Cortactin Is Not Needed for Tyrosine Phosphorylation of Syndecan-1—To examine the role of cortactin, we used siRNA to knock down this protein in cultured hepatocytes (Fig. 6*A*), followed by examination of each step that we have found in the syndecan endocytic pathway. As expected from the low levels of association from 5–15 min (Fig. 5, *A* and *B*), cortactin knockdown did not affect raft localization of FcR-Synd1 after clustering (data not shown). Remarkably, we found that cortactin knockdown abolished the ability of FcR-Synd1 or syndecan-1 to trigger Thr-202 or Tyr-204 phosphorylation of ERK after ligand binding (Fig. 6, *B–E*). Consistent with this finding, cortactin knockdown also stopped the loss of α-tubulin from FcR-Synd1 and syndecan-1 after ligand binding (Fig. 6, *F* and *G*). Because ERK activation and α-tubulin loss are rapid effects, these results suggest an early interaction of the

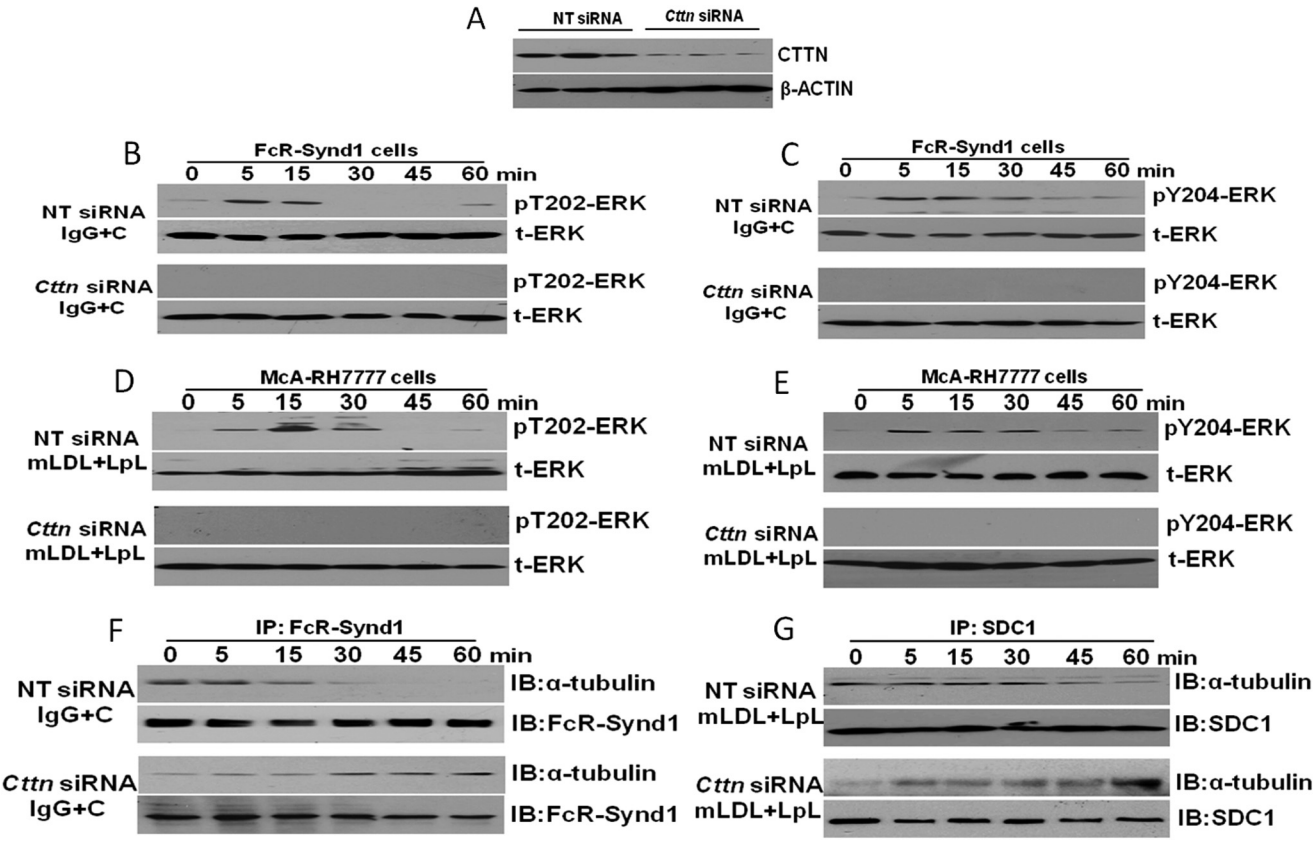

FIGURE 6. **Cortactin is required for rapid syndecan-mediated activation of ERK upon ligand binding and then ERK-dependent dissociation from α-tubulin.** *A,* efficacy of cortactin knockdown. McArdle cells expressing the FcR-Synd1 chimera were transfected with nontarget (*NT*) siRNA or rat cortactin (*Cttn*) siRNA. Displayed are immunoblots for cortactin and, as a loading control, β-actin. *B* and *C,* rapid activation of ERK stimulated by ligands for the FcR-Synd1 chimera requires cortactin. McArdle hepatocytes expressing the unmutated FcR-Synd1 chimera were transfected with nontarget or cortactin siRNAs as indicated, in parallel with the cells in *A*. Cells were chilled to 4 °C; unlabeled IgG was bound to the cell surface; unbound material was washed away, and then the cells were incubated at 37 °C for the indicated times in the presence of our clustering agent (+*C*). Displayed are immunoblots of cellular homogenates for phosphorylations of ERK at Thr-202 (*pT202-ERK*, *B*) and Tyr-204 (*pY204-ERK*, *C*). Immunoblots for total ERK (*t-ERK*) are also shown. *D* and *E,* rapid activation of ERK stimulated by ligands for syndecan-1 requires cortactin. McArdle hepatocytes expressing endogenous syndecan-1 were transfected with the indicated siRNAs. Knockdown of cortactin protein was verified, and then the cells were incubated with methylated LDL plus lipoprotein lipase (*mLDL+LpL*) at 37 °C for the indicated times. Displayed are immunoblots for phosphorylated (*C,* Thr(P)-202; *D,* Tyr(P)-204) and total ERK. *F,* release of α-tubulin from the FcR-Synd1 chimera after clustering requires cortactin. McArdle hepatocytes expressing the unmutated FcR-Synd1 chimera were treated as in *B* and *C*. Displayed are immunoprecipitations with anti-FcR antibodies (*IP: FcR-Synd1*), followed by immunoblots for α-tubulin (*IB: α-tubulin*) or the FcR ectodomain (*IB: FcR-Synd1*). *G,* release of α-tubulin from syndecan-1 after clustering requires cortactin. McArdle hepatocytes were treated as in *D* and *E*. Displayed are immunoprecipitations with anti-syndecan-1 antibodies (*IP: SDC1*), followed by immunoblots for α-tubulin (*IB: α-tubulin*) or syndecan-1 (*IB: SDC1*). The data are representative of a total of three independent knockdown experiments.

syndecan-1 cytoplasmic tail with cortactin that is not detected by co-immunoprecipitation or else an interaction of ERK with cortactin that is required for syndecan-1-mediated phosphorylations at Thr-202 and Tyr-204. Tyrosine phosphorylation after clustering of FcR-Synd1 and syndecan-1 still occurred after cortactin knockdown (Fig. 7, *A* and *B*). These data, in combination with the results in Fig. 5*E* and supplemental Fig. III, *G* and *H*, indicate that tyrosine phosphorylation causes cortactin recruitment, not the other way around. Finally, partial knockdown of cortactin inhibited efficient endocytosis of clustered ^{125}I-IgG by FcR-Synd1 and of LpL-enriched ^{125}I-mLDL by syndecan-1 (Fig. 7, *C* and *D*).

DISCUSSION

Our results provide the first detailed picture of sequential molecular events required for raft-dependent endocytosis. We examined the syndecan-1 HSPG after clustering induced by multivalent ligands. Its endocytosis can be divided into two phases, based on the kinase and the corresponding cytoskeletal partner that are involved. In the initial phase, ligands trigger rapid activation of ERK and localization of syndecan-1 into rafts (Fig. 8*A*). Syndecan-mediated activation of ERK depends on the MKKK motif and on the presence of cortactin. Raft localization requires clustering and cholesterol-rich microdomains, with no dependence on MKKK, ERK, Src family kinases, cortactin, or active cellular metabolism. Activation of ERK drives the dissociation of syndecan-1 from α-tubulin. Both α-tubulin and cortactin bind via the MKKK motif of syndecan-1, and loss of α-tubulin is required for efficient endocytosis, but persistent association with α-tubulin does not block cortactin recruitment. Instead, these results suggest that α-tubulin may act as an anchor for syndecan-1 at the plasma membrane in the basal state.

In the second phase, Src family kinases phosphorylate tyrosyl residues in the transmembrane and cytoplasmic region of syndecan-1, in a process that also requires the MKKK motif. We infer that these events are facilitated by the movement of clustered syndecan-1 into rafts (12), where Src family kinases are

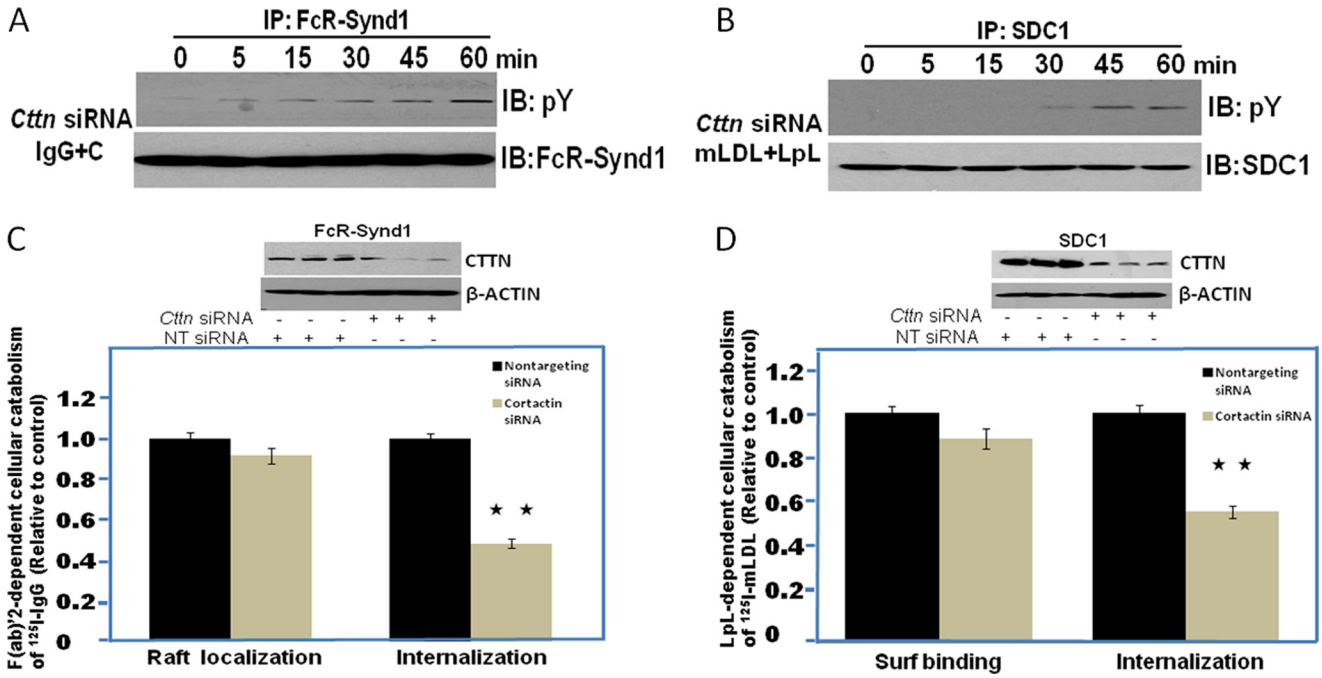

FIGURE 7. **Cortactin is not needed for tyrosine phosphorylation of syndecan-1 but is required for efficient endocytosis of FcR-Synd1 and syndecan-1 after clustering.** *A,* tyrosine phosphorylation of FcR-Synd1 after clustering does not require cortactin. McArdle hepatocytes expressing the unmutated FcR-Synd1 chimera were treated as in Fig. 6, *B* and *C*. Displayed are immunoprecipitations with anti-FcR antibodies (*IP: FcR-Synd1*), followed by immunoblots with antibodies against phosphotyrosine residues (*IB: pY*) or against the FcR ectodomain (*IB: FcR-Synd1*). *B,* tyrosine phosphorylation of syndecan-1 after clustering does not require cortactin. McArdle hepatocytes were treated as in Fig. 6, *D* and *E*. Displayed are immunoprecipitations with anti-syndecan-1 antibodies, followed by immunoblots for phosphotyrosines or syndecan-1. *C,* efficient endocytosis of FcR-Synd1 after clustering requires cortactin. McArdle hepatocytes expressing the unmutated FcR-Synd1 chimera were transfected with nontarget (*black columns*) or cortactin (*tan columns*) siRNAs. Partial knockdown of cortactin protein was verified in parallel wells (*inset*). After siRNA transfection, raft localization and internalization of ^{125}I-labeled IgG triggered by clustering were assessed after 1 h at 37 °C, as in Fig. 1. Displayed are clustering-dependent raft localization and internalization of ligand, normalized to control values from cells expressing the unmutated chimera (mean ± S.E., $n = 3$; non-normalized control values were 510 ± 18.16 and 482 ± 13.6 ng/mg, respectively). *D,* efficient syndecan-1-mediated endocytosis after clustering requires cortactin. McArdle hepatocytes were transfected with nontarget (*black columns*) or cortactin (*tan columns*) siRNAs. After siRNA transfection, cells were incubated for 1 h at 37 °C with ^{125}I-labeled mLDL, without or with LpL. Displayed are LpL-dependent surface (*Surf*) binding and internalization of ligand, normalized to control values from cells receiving nontarget siRNA (mean ± S.E., $n = 3$; non-normalized control values were 301.27 ± 11.26 and 542.07 ± 19.14 ng/mg, respectively). **, $p < 0.01$ (two-tailed Student's *t* test, *C* and *D*). The data are representative of a total of three independent IP/IB and ligand catabolism experiments.

present (34). Rafts also provide an environment shielded from transmembrane tyrosine phosphatases (35). Tyrosine phosphorylation of syndecan-1 triggers the robust recruitment of cortactin, which we found to be an essential mediator of efficient actin-dependent endocytosis (Fig. 8*B*).

Several aspects of this endocytic pathway could allow for physiologic regulation. First, a rate-limiting step appears to be Src-mediated tyrosine phosphorylation of syndecan-1, which almost immediately causes robust cortactin recruitment and endocytosis (Figs. 4*F* and 5 and supplemental Fig. III, *G* and *H*). Thus, processes that enhance tyrosine phosphorylation or inhibit tyrosine phosphatases might accelerate syndecan-1-mediated endocytosis. An attractive candidate is insulin, which is released in the postprandial state, activates the tyrosine kinase activity of the insulin receptor, activates ERK, and stimulates NOX4 to disable protein-tyrosine phosphatases (28, 36, 37). Other growth factors produce similar effects (38), and cytokines, additional enzymes, chaperones, and other ancillary molecules may also participate (5, 39–42). Second, the need for clustering to trigger specific steps in syndecan-1-mediated endocytosis could allow the system to sense ligand size, valence, binding affinity, and potentially other characteristics. Consistent with this idea, our previous side-by-side comparison showed that a larger ligand, VLDL, underwent more rapid catabolism than did a smaller ligand, LpL-enriched mLDL (see page 1963 of Ref. 16). Moreover, a series of artificial ligands that recognize different sulfation epitopes on the heparan sulfate side chains of syndecans bound similarly to the cell surface, but only a strong ligand for 2-*O*-sulfated groups drove endocytosis, presumably by triggering clustering and membrane invagination (43). Third, we previously reported that regulated secretion of molecules, particularly sulfatase-2 (SULF2), that enzymatically modify or sterically hinder the binding domains on the heparan sulfate side chains of syndecan-1 can alter ligand catabolism *in vitro* and *in vivo* (16, 20, 44, 45). Fourth, co-operation with other raft-associated receptors, such as SR-BI or clustered glypicans, could also affect ligand trafficking (20, 43).

This detailed characterization of ligand handling by syndecan-1 also sheds light on disease. For example, syndecans, including syndecan-1, have been shown to facilitate infection of human macrophages with HIV-1 (46, 47). Presumably, the virus acts as a multivalent ligand, driving syndecan into rafts, which other studies have shown to be the preferred site for fusion of the HIV-1 envelope with the target cell membrane, to allow infectious entry (48–50). Syndecans appear ideally suited for hijacking by HIV-1, because the ~1-h delay between their rapid movement into rafts and subsequent endocytosis would allow time for envelope fusion and hence infection to occur, before

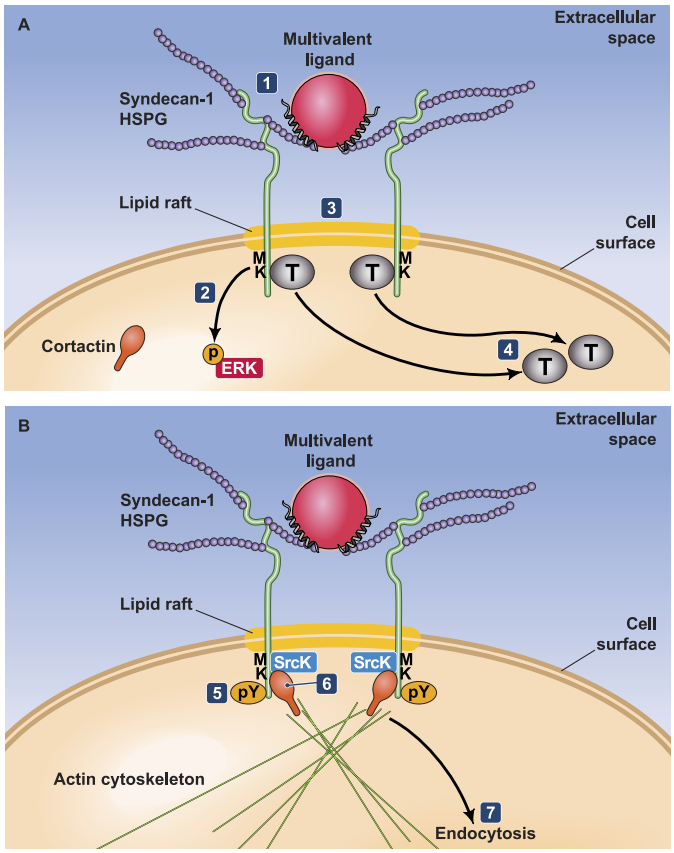

FIGURE 8. **Two distinct phases in raft-dependent endocytosis of syndecan-1, a conserved multifunctional receptor.** *A,* rapid initial phase of syndecan-1 endocytosis. Ligand binding (*1*) triggers rapid activation of ERK (*2*), and clustering drives the movement of syndecan-1 into rafts (*3*). Activation of ERK depends on the syndecan-1 MKKK motif and on the presence of cortactin within the cell. Raft localization requires cholesterol-rich membrane microdomains (*thickened yellow region* of the cell surface), with no dependence on MKKK, ERK, Src family kinases, cortactin, or active cellular metabolism. Activation of ERK drives the dissociation of syndecan-1 from α-tubulin (*T*), a molecule that we speculate may act as an anchor for syndecan-1 at the plasma membrane in the basal state (*4*). *B,* second phase of syndecan-1 endocytosis. Clustering of the syndecan-1 cytoplasmic MKKK motif gradually triggers Src-dependent phosphorylation of conserved tyrosyl residues within the syndecan-1 transmembrane and cytoplasmic domains (*5*), which in turn causes the robust recruitment of cortactin (*6*) and then efficient actin-dependent endocytosis (*7*). Abbreviations: *MK,* MKKK motif; *p,* phosphorylation; *pY,* tyrosyl phosphorylation; *SrcK,* Src family kinases; *T,* α-tubulin. The polypeptide backbone (core protein) of the syndecan-1 HSPG is drawn in *light green*, and the heparan sulfate side chains are denoted by chains of *small ovals*. The helices on the surface of the multivalent ligand represent protein elements, such as gp120 or lipoprotein lipase, that bind the heparan sulfate side-chains of syndecan-1.

syndecans can deliver the viral ligand into lysosomes for hydrolysis and sterilization. We infer that the preferential binding of the HIV-1 envelope glycoprotein gp120 to 6-*O*-sulfated groups over 2-*O*-sulfated groups on syndecans (47) may further delay endocytosis (43), thereby favoring infectious entry via fusion with cellular rafts. Moreover, ligand binding to syndecan-1 activates ERK, and ERK activation has been shown to facilitate HIV-1 infectivity and the assembly and release of new virions (51, 52).

We (11–13) and others (53) have demonstrated a crucial role for syndecan-1 in the safe hepatic disposal of atherogenic postprandial remnant lipoproteins, thereby resolving a long-standing controversy over the identity of the receptors responsible for this important pathway. Syndecan-1 is abundantly expressed on the sinusoidal surface of hepatic parenchymal cells (54, 55), along microvilli facing the space of Disse (53), where remnant lipoproteins are cleared (11, 13, 20). Knowledge of the syndecan-1 endocytic pathway has already allowed us to identify specific molecular defects that impair its function in type 1 and type 2 diabetes mellitus and may thereby contribute to dyslipoproteinemia and increased cardiovascular risk in those conditions (16, 20, 45, 56). Our current results indicate additional points of control (Fig. 8) and may facilitate future studies on how the healthy liver handles the lipid load from remnant lipoproteins that it internalizes via syndecan-1. In diabetic dyslipoproteinemia and other conditions, continuously high levels of ligands for syndecan-1, such as remnant lipoproteins or sulfatase-2, may cause aberrant activation or desensitization of ERK or Src family kinases, with downstream effects. Syndecans may also mediate uptake of cholesterol-rich aggregated lipoproteins by macrophages within the arterial wall, leading to the formation of foam cells, a hallmark of atherosclerosis (57).

Differences among raft-dependent receptors emphasize the need for precise molecular characterizations of each. As noted above, SV40 enters via rafts for delivery to the endoplasmic reticulum, whereas syndecan-1 enters via rafts and carries its ligands to lysosomes for destruction (11, 12). Although Src was one of six major kinases identified in SV40 endocytosis (58), the generalizability of findings from that system to any other raft-dependent receptor will need to be tested. Of note, the MKKK motif appears, with one conservative substitution, in the juxtamembrane region of the *Drosophila* syndecan cytoplasmic tail (MRKK) (18). The same single conservative substitution is present in human syndecan-2, which also mediates endocytosis under some circumstances (11), suggesting considerable biologic importance of this novel motif.

Overall, our findings provide new insights into raft-mediated endocytosis by a highly conserved receptor, syndecan-1, and they will facilitate additional studies into its roles in ligand binding, downstream signaling, endocytosis, and other trafficking in normal and diseased states.

REFERENCES

1. Nichols, B. J., and Lippincott-Schwartz, J. (2001) Endocytosis without clathrin coats. *Trends Cell Biol.* **11,** 406–412
2. Anderson, R. G., and Jacobson, K. (2002) A role for lipid shells in targeting proteins to caveolae, rafts, and other lipid domains. *Science* **296,** 1821–1825
3. Kirkham, M., and Parton, R. G. (2005) Clathrin-independent endocytosis: new insights into caveolae and noncaveolar lipid raft carriers. *Biochim. Biophys. Acta* **1745,** 273–286
4. Römer, W., Pontani, L. L., Sorre, B., Rentero, C., Berland, L., Chambon, V., Lamaze, C., Bassereau, P., Sykes, C., Gaus, K., and Johannes, L. (2010) Actin dynamics drive membrane reorganization and scission in clathrin-independent endocytosis. *Cell* **140,** 540–553
5. Pelkmans, L., Fava, E., Grabner, H., Hannus, M., Habermann, B., Krausz, E., and Zerial, M. (2005) Genome-wide analysis of human kinases in clathrin- and caveolae/raft-mediated endocytosis. *Nature* **436,** 78–86
6. Kartenbeck, J., Stukenbrok, H., and Helenius, A. (1989) Endocytosis of simian virus 40 into the endoplasmic reticulum. *J. Cell Biol.* **109,** 2721–2729
7. Stang, E., Kartenbeck, J., and Parton, R. G. (1997) Major histocompatibility complex class I molecules mediate association of SV40 with caveolae. *Mol.*

Biol. Cell **8,** 47–57
8. Bonifacino, J. S., and Traub, L. M. (2003) Signals for sorting of transmembrane proteins to endosomes and lysosomes. *Annu. Rev. Biochem.* **72,** 395–447
9. Michaely, P., Zhao, Z., Li, W. P., Garuti, R., Huang, L. J., Hobbs, H. H., and Cohen, J. C. (2007) Identification of a VLDL-induced, FDNPVY-independent internalization mechanism for the LDLR. *EMBO J.* **26,** 3273–3282
10. Benmerah, A., and Lamaze, C. (2007) Clathrin-coated pits: vive la différence? *Traffic* **8,** 970–982
11. Fuki, I. V., Kuhn, K. M., Lomazov, I. R., Rothman, V. L., Tuszynski, G. P., Iozzo, R. V., Swenson, T. L., Fisher, E. A., and Williams, K. J. (1997) The syndecan family of proteoglycans: novel receptors mediating internalization of atherogenic lipoproteins *in vitro*. *J. Clin. Invest.* **100,** 1611–1622
12. Fuki, I. V., Meyer, M. E., and Williams, K. J. (2000) Transmembrane and cytoplasmic domains of syndecan mediate a multistep endocytic pathway involving detergent-insoluble membrane rafts. *Biochem. J.* **351,** 607–612
13. Williams, K. J., and Fuki, I. V. (1997) Cell-surface heparan sulfate proteoglycans: dynamic molecules mediating ligand catabolism. *Curr. Opin. Lipidol.* **8,** 253–262
14. Bernfield, M., Götte, M., Park, P. W., Reizes, O., Fitzgerald, M. L., Lincecum, J., and Zako, M. (1999) Functions of cell surface heparan sulfate proteoglycans. *Annu. Rev. Biochem.* **68,** 729–777
15. Gingis-Velitski, S., Zetser, A., Kaplan, V., Ben-Zaken, O., Cohen, E., Levy-Adam, F., Bashenko, Y., Flugelman, M. Y., Vlodavsky, I., and Ilan, N. (2004) Heparanase uptake is mediated by cell membrane heparan sulfate proteoglycans. *J. Biol. Chem.* **279,** 44084–44092
16. Chen, K., Liu, M.-L., Schaffer, L., Li, M., Boden, G., Wu, X., and Williams, K. J. (2010) Type 2 diabetes in mice induces hepatic overexpression of sulfatase 2, a novel factor that suppresses uptake of remnant lipoproteins. *Hepatology* **52,** 1957–1967
17. Sarrazin, S., Lamanna, W. C., and Esko, J. D. (2011) Heparan sulfate proteoglycans. *Cold Spring Harbor Perspect. Biol.* **3,** a004952
18. Spring, J., Paine-Saunders, S. E., Hynes, R. O., and Bernfield, M. (1994) *Drosophila* syndecan: Conservation of a cell-surface heparan sulfate proteoglycan. *Proc. Natl. Acad. Sci. U.S.A.* **91,** 3334–3338
19. Zimmermann, P., and David, G. (1999) The syndecans, tuners of transmembrane signaling. *FASEB J.* **13,** S91–S100
20. Williams, K. J., and Chen, K. (2010) Recent insights into factors affecting remnant lipoprotein uptake. *Curr. Opin. Lipidol.* **21,** 218–228
21. Granés, F., Berndt, C., Roy, C., Mangeat, P., Reina, M., and Vilaró, S. (2003) Identification of a novel ezrin-binding site in syndecan-2 cytoplasmic domain. *FEBS Lett.* **547,** 212–216
22. Chakravarti, R., Sapountzi, V., and Adams, J. C. (2005) Functional role of syndecan-1 cytoplasmic V region in lamellipodial spreading, actin bundling, and cell migration. *Mol. Biol. Cell* **16,** 3678–3691
23. Grootjans, J. J., Zimmermann, P., Reekmans, G., Smets, A., Degeest, G., Dürr, J., and David, G. (1997) Syntenin, a PDZ protein that binds syndecan cytoplasmic domains. *Proc. Natl. Acad. Sci. U.S.A.* **94,** 13683–13688
24. Cohen, A. R., Woods, D. F., Marfatia, S. M., Walther, Z., Chishti, A. H., and Anderson, J. M. (1998) Human CASK/LIN-2 binds syndecan-2 and protein 4.1 and localizes to the basolateral membrane of epithelial cells. *J. Cell Biol.* **142,** 129–138
25. Zimmermann, P., Zhang, Z., Degeest, G., Mortier, E., Leenaerts, I., Coomans, C., Schulz, J., N'Kuli, F., Courtoy, P. J., and David, G. (2005) Syndecan recycling is controlled by syntenin-PIP2 interaction and Arf6. *Dev. Cell* **9,** 377–388
26. Chen, K., Liu, M.-L., and Williams, K. J. (2008) Molecular determinants of endocytosis and tyrosine phosphorylation within the cytoplasmic tail of human syndecan-1, a receptor for remnant lipoproteins. *Circulation* **118,** S_453
27. Chen, K., and Williams, K. J. (2011) Tyrosine phosphorylation of syndecan-1, a receptor for remnant lipoproteins, triggers its binding to cortactin, an essential intracellular mediator of a novel endocytic pathway. *Circulation* **124,** A10838
28. Wu, X., and Williams, K. J. (2012) NOX4 pathway as a source of selective insulin resistance and responsiveness. *Arterioscler. Thromb. Vasc. Biol.* **32,** 1236–1245
29. Williams, K. J. (2001) Interactions of lipoproteins with proteoglycans. *Methods Mol. Biol.* **171,** 457–477
30. Rauch, B. H., Millette, E., Kenagy, R. D., Daum, G., Fischer, J. W., and Clowes, A. W. (2005) Syndecan-4 is required for thrombin-induced migration and proliferation in human vascular smooth muscle cells. *J. Biol. Chem.* **280,** 17507–17511
31. Li, X., Herz, J., and Monard, D. (2006) Activation of ERK signaling upon alternative protease nexin-1 internalization mediated by syndecan-1. *J. Cell Biochem.* **99,** 936–951
32. Kinnunen, T., Kaksonen, M., Saarinen, J., Kalkkinen, N., Peng, H. B., and Rauvala, H. (1998) Cortactin-Src kinase signaling pathway is involved in N-syndecan-dependent neurite outgrowth. *J. Biol. Chem.* **273,** 10702–10708
33. Cosen-Binker, L. I., and Kapus, A. (2006) Cortactin: the gray eminence of the cytoskeleton. *Physiology* **21,** 352–361
34. Rothberg, K. G., Heuser, J. E., Donzell, W. C., Ying, Y. S., Glenney, J. R., and Anderson, R. G. (1992) Caveolin, a protein component of caveolae membrane coats. *Cell* **68,** 673–682
35. Holowka, D., Gosse, J. A., Hammond, A. T., Han, X., Sengupta, P., Smith, N. L., Wagenknecht-Wiesner, A., Wu, M., Young, R. M., and Baird, B. (2005) Lipid segregation and IgE receptor signaling: a decade of progress. *Biochim. Biophys. Acta* **1746,** 252–259
36. Mahadev, K., Motoshima, H., Wu, X., Ruddy, J. M., Arnold, R. S., Cheng, G., Lambeth, J. D., and Goldstein, B. J. (2004) The NAD(P)H oxidase homolog Nox4 modulates insulin-stimulated generation of H_2O_2 and plays an integral role in insulin signal transduction. *Mol. Cell. Biol.* **24,** 1844–1854
37. Wu, X., Chen, K., and Williams, K. J. (2012) The role of pathway-selective insulin resistance and responsiveness in diabetic dyslipoproteinemia. *Curr. Opin. Lipidol.* **23,** 334–344
38. Rhee, S. G., Kang, S. W., Jeong, W., Chang, T. S., Yang, K. S., and Woo, H. A. (2005) Intracellular messenger function of hydrogen peroxide and its regulation by peroxiredoxins. *Curr. Opin. Cell Biol.* **17,** 183–189
39. Liberali, P., Rämö, P., and Pelkmans, L. (2008) Protein kinases: starting a molecular systems view of endocytosis. *Annu. Rev. Cell Dev. Biol.* **24,** 501–523
40. Ingley, E. (2008) Src family kinases: regulation of their activities, levels, and identification of new pathways. *Biochim. Biophys. Acta* **1784,** 56–65
41. Wittrup, A., Zhang, S. H., Svensson, K. J., Kucharzewska, P., Johansson, M. C., Mörgelin, M., and Belting, M. (2010) Magnetic nanoparticle-based isolation of endocytic vesicles reveals a role of the heat shock protein GRP75 in macromolecular delivery. *Proc. Natl. Acad. Sci. U.S.A.* **107,** 13342–13347
42. Giannoni, E., Taddei, M. L., and Chiarugi, P. (2010) Src redox regulation: again in the front line. *Free Radic. Biol. Med.* **49,** 516–527
43. Wittrup, A., Zhang, S. H., ten Dam, G. B., van Kuppevelt, T. H., Bengtson, P., Johansson, M., Welch, J., Mörgelin, M., and Belting, M. (2009) ScFv antibody-induced translocation of cell-surface heparan sulfate proteoglycan to endocytic vesicles: evidence for heparan sulfate epitope specificity and role of both syndecan and glypican. *J. Biol. Chem.* **284,** 32959–32967
44. Williams, K. J. (2008) Molecular processes that handle– and mishandle–dietary lipids. *J. Clin. Invest.* **118,** 3247–3259
45. Hassing, H. C., Mooij, H., Guo, S., Monia, B. P., Chen, K., Kulik, W., Dallinga-Thie, G. M., Nieuwdorp, M., Stroes, E. S., and Williams, K. J. (2012) Inhibition of hepatic sulfatase-2 *in vivo*: A novel strategy to correct diabetic dyslipidemia. *Hepatology* **55,** 1746–1753
46. Saphire, A. C., Bobardt, M. D., Zhang, Z., David, G., and Gallay, P. A. (2001) Syndecans serve as attachment receptors for human immunodeficiency virus type 1 on macrophages. *J. Virol.* **75,** 9187–9200
47. de Parseval, A., Bobardt, M. D., Chatterji, A., Chatterji, U., Elder, J. H., David, G., Zolla-Pazner, S., Farzan, M., Lee, T. H., and Gallay, P. A. (2005) A highly conserved arginine in gp120 governs HIV-1 binding to both syndecans and CCR5 via sulfated motifs. *J. Biol. Chem.* **280,** 39493–39504
48. Mañes, S., del Real, G., Lacalle, R. A., Lucas, P., Gómez-Moutón, C., Sánchez-Palomino, S., Delgado, R., Alcamí, J., Mira, E., and Martínez-A, C. (2000) Membrane raft microdomains mediate lateral assemblies required for HIV-1 infection. *EMBO Rep.* **1,** 190–196
49. Liao, Z., Cimakasky, L. M., Hampton, R., Nguyen, D. H., and Hildreth, J. E.

(2001) Lipid rafts and HIV pathogenesis: host membrane cholesterol is required for infection by HIV type 1. *AIDS Res. Hum. Retroviruses* **17,** 1009–1019
50. Rawat, S. S., Viard, M., Gallo, S. A., Blumenthal, R., and Puri, A. (2006) Sphingolipids, cholesterol, and HIV-1: a paradigm in viral fusion. *Glycoconj. J.* **23,** 189–197
51. Yang, X., and Gabuzda, D. (1999) Regulation of human immunodeficiency virus type 1 infectivity by the ERK mitogen-activated protein kinase signaling pathway. *J. Virol.* **73,** 3460–3466
52. Furler, R. L., and Uittenbogaart, C. H. (2010) Signaling through the p38 and ERK pathways: a common link between HIV replication and the immune response. *Immunol. Res.* **48,** 99–109
53. Stanford, K. I., Bishop, J. R., Foley, E. M., Gonzales, J. C., Niesman, I. R., Witztum, J. L., and Esko, J. D. (2009) Syndecan-1 is the primary heparan sulfate proteoglycan mediating hepatic clearance of triglyceride-rich lipoproteins in mice. *J. Clin. Invest.* **119,** 3236–3245
54. Hayashi, K., Hayashi, M., Jalkanen, M., Firestone, J. H., Trelstad, R. L., and Bernfield, M. (1987) Immunocytochemistry of cell surface heparan sulfate proteoglycan in mouse tissue. A light and electron microscopic study. *J. Histochem. Cytochem.* **35,** 1079–1088
55. Roskams, T., Moshage, H., De Vos, R., Guido, D., Yap, P., and Desmet, V. (1995) Heparan sulfate proteoglycan expression in normal human liver. *Hepatology* **21,** 950–958
56. Williams, K. J., Liu, M.-L., Zhu, Y., Xu, X., Davidson, W. R., McCue, P., and Sharma, K. (2005) Loss of heparan *N*-sulfotransferase in diabetic liver: role of angiotensin II. *Diabetes* **54,** 1116–1122
57. Boyanovsky, B. B., Shridas, P., Simons, M., van der Westhuyzen, D. R., and Webb, N. R. (2009) Syndecan-4 mediates macrophage uptake of group V secretory phospholipase A_2-modified low density lipoprotein. *J. Lipid Res.* **50,** 641–650
58. Pelkmans, L., and Zerial, M. (2005) Kinase-regulated quantal assemblies and kiss-and-run recycling of caveolae. *Nature* **436,** 128–133